Application of dual-emission laser induced fluorescence technique on pH measurement around different size bubbles

Conference Paper

Author(s):
Kong, G.; Buist, K.A.; Peters, E.A.J.F.; Kuipers, J.A.M.

APPLICATION OF DUAL-EMISSION LASER INDUCED FLUORESCENCE TECHNIQUE ON PH MEASUREMENT AROUND DIFFERENT SIZE BUBBLES

G. Kong[1,c], K.A. Buist[1], E.A.J.F. Peters[1], J.A.M. Kuipers[1]

[1]Multiphase Reactors group, Department of Chemical Engineering & Chemistry, Eindhoven University of Technology, P.O. box 513, 5600 MB Eindhoven, The Netherlands
[c]Corresponding author: Tel.: +31 40 247 8199; Email: g.kong@tue.nl

KEYWORDS:

Main subjects: mass transfer, flow visualization
Fluid: water/CO_2 bubble
Visualization method(s): Laser Induced Fluorescence

ABSTRACT: *A dual-emission Laser Induced Fluorescence technique is applied to pH fields around single rising bubbles. The advantage of this technique allows us to quantify the pH field around the single rising bubbles. Varied sizes of bubble ranging 0.7mm-3.5mm are visualized to investigate the size effect on the distribution of the transferred mass.*

1 Introduction

Mass transfer is the core process in chemical engineering. It is the essential knowledge for improving the reactor design. As a kind of chemical reactor, bubble column reactors have been developed for realizing the multiphase reaction due to their good mixing and long contact time properties of mass transfer process. The mass transfer dynamics in bubble reactors have attracted great attention of researchers. Gogate and Pandit (1999) reviewed varied methods on global mass transfer in bubbly flow. On the other hand, the details of mass transfer are highly desired. Techniques for local mass transfer measurement emergence with the progress of concerning technologies, such as lasers, cameras and tracers.

As a flow visualization technique, laser induced fluorescence has become a promising technique in gas-liquid interface mass transfer. A lot of effort has been made to prompt the progress. So far, two typical laser induced fluorescence techniques are involved in bubble mass transfer investigation, including O_2 quenching technique (Bork, Dani, Dietrich, Francois, Jimenez) and CO_2/ pH sensitive technique (Pankow, Asher, Munsterer, Jahne, Tsuchiya,Stohr, Valiorgue, Kovats). Recently, Paul et al (2018) reviewed the overview of the technique development.

A more advanced technique has been develop recently for mass transfer of CO_2 bubbles in water (Kong et al 2018) devoting to quantitative measurement. The dual-emission laser induced fluorescence technique (DLIF) delicately combines a dual-emission fluorescent dye and laser induced fluorescence technique. The normalization of those two bands overcomes the non-uniformness of illumination intensity. This principle basically allows us to quantitatively the transferred mass around bubbles. The principle formula reads

$$\alpha(pH) = \frac{I_{\lambda_1 f}(\lambda_1, pH)}{I_{\lambda_2 f}(\lambda_2, pH)} = \frac{I_0 e^{-\epsilon(pH)lc} A\Phi(\lambda_1, pH)C\epsilon(pH)l}{I_0 e^{-\epsilon(pH)lc} A\Phi(\lambda_2, pH)C\epsilon(pH)l} \propto \frac{\Phi(\lambda_1, pH)}{\Phi(\lambda_2, pH)}$$

in which, I_0 is the incident light intensity, ϵ is the absorption (extinction) coefficient, λ_{La} is the incident light wavelength, l is the optical path length of the incident ray, L the length of the sampling volume, A is the optical collection fraction, C is the fluorescence concentration and Φ is the quantum yield.

In this study, the dual-emission LIF technique is applied to a water/CO_2 system. The pH fields around a single rising CO_2 bubble with varied size (0.7mm-3.5mm) are measured to visualize the size effect of bubbles on gas-liquid mass transfer.

2 Setup and device

The setup comprises one bubble column made of glass (dimensions: 10 cm✕10 cm✕40 cm), two imager sCMOS cameras with 2560✕2160 pixel and a maximum frame rate of 50 Hz at full resolution equipped with Tokina 100mm F/2.8 Marco AT-X lenses and a pulsed Nd:Yag laser (Litron LPY-70-200) with 200 Hz maximum pulse frequency and maximum energy of 50 mJ. Additionally, two optics including one spherical lens and a f/-20 mm cylindrical Plano-Concave lens are mounted to generate the laser sheet. Two optical filters are applied for the cameras to isolate the light signal corresponding to two spectral bands (as shown in figure 1); 575/50 nm for camera 1 and 650/80 nm for camera 2. A dual-emission fluorescent dye is selected as the pH indicator, which is 1, 4(and 5)-benzenedicarboxylic acid, 2-[10-(dimethylamino)-4-fluoro- 3-oxo-3H-benzo[c]xanthen-7-yl] (C-SNARF-4F). The performance of the dye has been demonstrated in (Kong et al 2018). The concentration of dye used in this study is $1.06 \times 10^{-6}\ mol/L$ ($0.5\ mg/L$). The recording and post-processing are implemented with DaVis 8.3.0 (LaVision). In practise to obtain a higher temporal resolution, the recording area is cropped (702✕2560), allowing a recording frame rate of 100 Hz, the exposure time is kept at 1 ms. The system is adjusted properly to yield a spatial resolution of 0.0133mm/pixel. This grants us the ability to capture the details of small bubbles (<1mm) and big enough domain of big bubbles (>2mm).
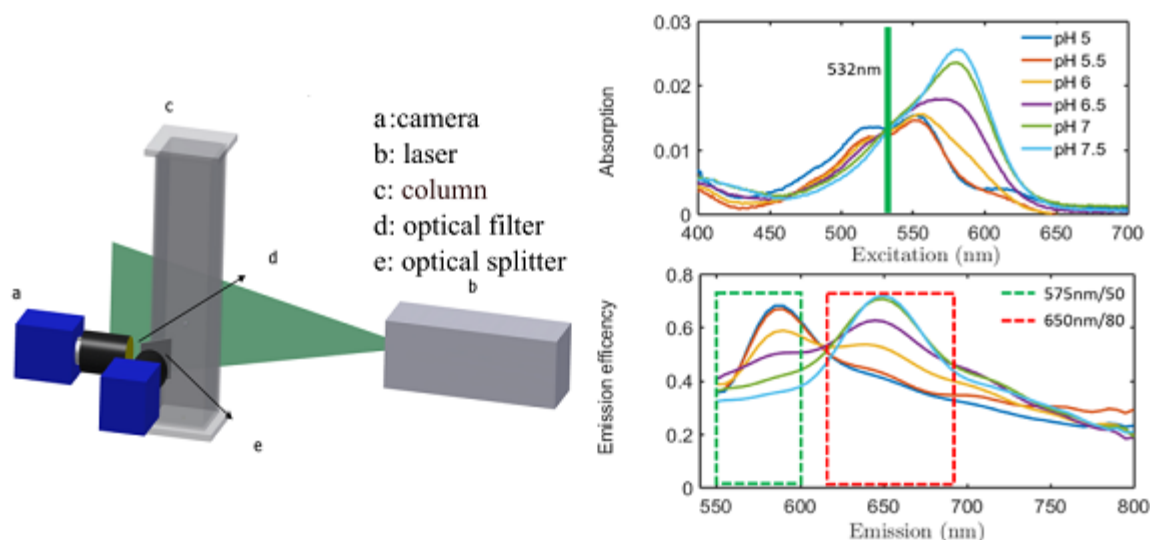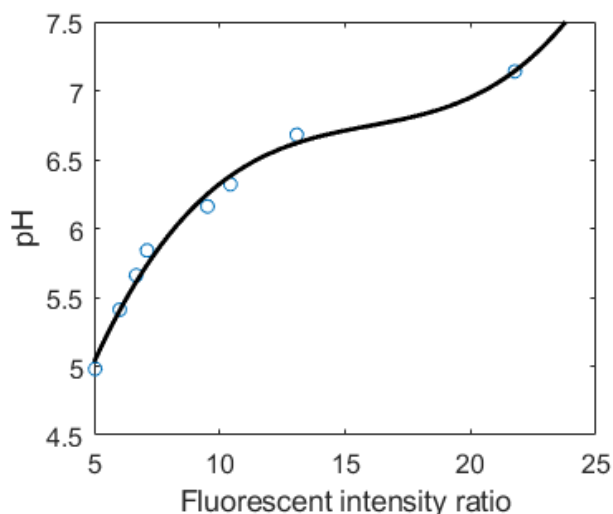

Figure 1: setup (left); dye emission spectral (right)

Figure 2: Calibration of relation between pH and fluorescence intensity ratio

To obtain the relation between pH and fluorescent intensity ratio, a pH calibration is required. The image recording is implemented under the same conditions as those for the experimental images. The pH is adjusted with $Citric\ acid - Na_2HPO_4$ buffer solutions. As demonstrated in Kong et al (2018), the over-all uncertainty of pH measurement is around 0.02 pH units, while an upper bound of 0.04 pH units.

The image post processing follows a procedure as shown in figure 3, for conciseness sake, the details are not discussed here and can be found in Kong et al (2018).
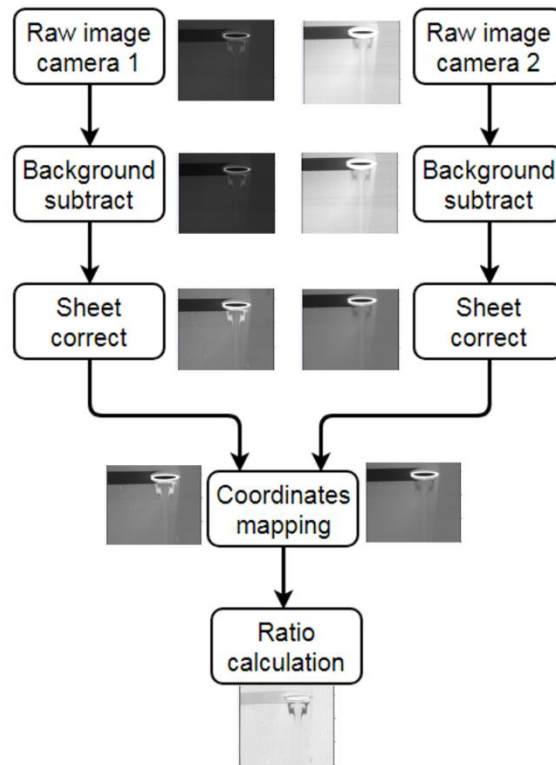
Figure 3: Image post processing flow diagram.

3 Results

According to Grace Diagram, in water system, bubbles smaller than 1mm rise straight and keep spherical shape; bubbles bigger than 2mm, the rising paths are no longer straight and bubbles are in wobbling regime. Both the rising behaviour and shape affect the mass transfer. Therefore, varied size bubbles are generated to investigate the effect of the shape and rising behaviour on the mass transfer.

In this study, bubbles of sizes 0.7mm, 1.1mm, 2.6mm and 3.5mm are generated. The pH fields around the rising bubbles are obtained via the dual-emission LIF technique. Please note that the background pH changes due to dissolved CO_2. For better visualization sake, the Colormaps on pH contour images change slightly. pH contour images are overlaid masks of bubbles to avoid the distraction of nonsense value. Note also that the masks don't represent the real bubble due to the fact that bubble surface are hard to determine because of laser reflection caused halo around the bubble surface.

3.1 Bubble size, 0.7mm.

The shape of bubble of size 0.7mm is spherical and the Reynolds number is around 100. Therefore, the rising path is straight. The rising dynamic and mass transfer reach the static stage in short time. Thus only one figure is shown here. The concentration of dissolved mass is indicated by the pH. The pH distribution shows that most of the mass is in the core of the wake. The amount of mass declines gradually as the distance increases away from the bubble surface in the wake.
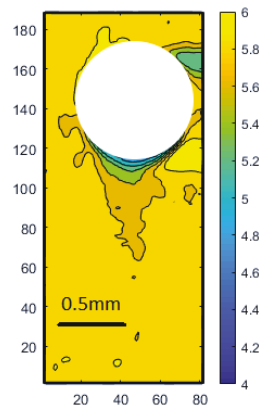
Figure 4: pH around a 0.7mm rising bubble

3.2 Bubble size, 1.1mm

For size 1.1 mm bubble, the Reynolds is around 200 and the shape is spherical. The rising path should be straight. However, the rising path deviates due to the effect of leading bubble. For the same reason as 0.7mm bubbles, only one images is shown here. The pH distribution is similar with 0.7 mm bubbles. However, a neck is observed separating a high mass region from the vicinity of bubble surface.
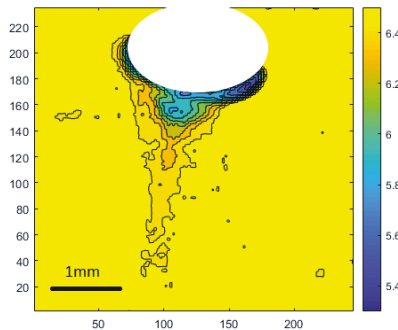

Figure 5: pH around a 1.1 mm rising bubble

3.3 Bubble size, 2.6mm

For 2.6mm size bubble, the Reynolds number is around 800. The bubble is in wobbling regime according to grace diagram. Therefore, the shape is ellipsoidal. In the wake of the rising bubble, vortex shedding occurs. As shown in Figure 6, dissolved mass firstly is accumulated in the wake and transported with the vortex shedding. The wake is relatively stable with periodic vortex shedding. As indicated by the pH, the concentration of the mass is higher in the core of wake and the higher concentration regions are always located in the core of vortices. The vortices divide the mass zone into two main parts. Each one has its own higher concentration core.
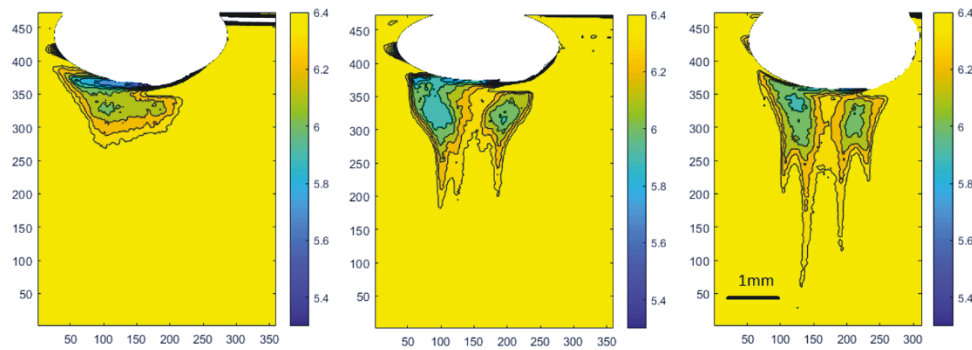
Figure 6: pH around a 2.6 mm rising bubble. The time interval between the images are 10ms.

3.4 Bubble size, 3.5mm

Bubbles of size 3.5 mm are rising in high Reynolds number regime. The Reynolds number is around 1000. The shape of bubbles is strongly deformed. High Reynolds number and highly deformed shape result in a wake rapid evolving into distorted wake. Most of the mass is located in the core region of the vortices at the early stage. Later on, compared with 2.5 mm bubble, for which pH distribution is still within the two main vortexes, pH distribution of size 3.5 mm is mainly at the outer edge of the bubble wake. This is clearly shown in Figure 7 and 8 in different angle of recording.
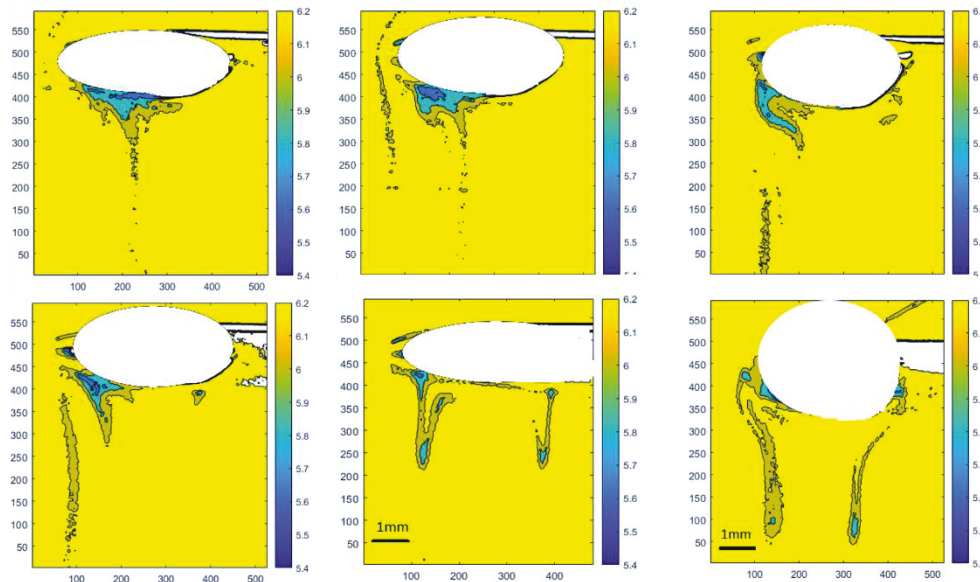

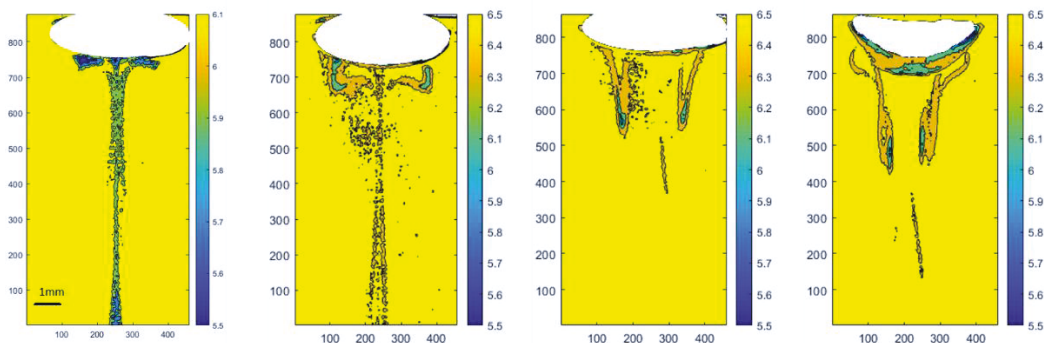**Figure 7: pH around a 3.5 mm rising bubble. The time interval between the images are 10ms.**

Figure 8: pH around a 3.5 mm rising bubble (another angle). The time interval between the images are 10ms.

Conclusion

A recently developed quantitative technique, dual-emission Laser Induced Fluorescence technique (DLIF), is applied to varied size of bubbles. The size range is between 0.7mm-3.5mm. The pH field as an indication of transferred mass are observed by this DLIF technique. The results show that the distributions of dissolved mass of different size bubble are pretty different.

Acknowledgement

Reference

Gogate, P.R., Pandit, A.B., 1999. Survey of measurement techniques for gas–liquid mass transfer coefficient in bioreactors. Biochem. Eng. J. 4, 7–15. doi:10.1016/S1369-703X(99)00033-9

Bork, O., Schlueter, M. and Raebiger, N. 2005, The Impact of Local Phenomena on Mass Transfer in Gas-Liquid Systems. Can. J. Chem. Eng., 83: 658–666. doi:10.1002/cjce.5450830406

Dani, A., Guiraud, P., Cockx, A., 2007. Local measurement of oxygen transfer around a single bubble by planar laser-induced fluorescence. Chem. Eng. Sci. 62, 7245–7252. doi:10.1016/j.ces.2007.08.047

Dietrich, N., Francois, J., Jimenez, M., Cockx, A., Guiraud, P., Hébrard, G., 2015. Fast Measurements of the Gas-Liquid Diffusion Coefficient in the Gaussian Wake of a Spherical Bubble. Chem. Eng. Technol. 38, 941–946. doi:10.1002/ceat.201400471

Francois, J., Dietrich, N., Guiraud, P., Cockx, A., 2011. Direct measurement of mass transfer around a single bubble by micro-PLIFI. Chem. Eng. Sci. 66, 3328–3338. doi:10.1016/j.ces.2011.01.049

Jimenez, M., Dietrich, N., Hébrard, G., 2013. Mass transfer in the wake of non-spherical air bubbles quantified by quenching of fluorescence. Chem. Eng. Sci. 100, 160–171. doi:10.1016/j.ces.2013.01.036

Marcotte, N., Brouwer, A.M., 2005. Carboxy SNARF-4F as a Fluorescent pH Probe for Ensemble and Fluorescence Correlation Spectroscopies. J. Phys. Chem. B 109, 11819–11828. doi:10.1021/jp0510138

Münsterer, T., Jähne.B., 1998. LIF measurements of concentration profiles in the aqueous mass boundary layer. Exp. Fluids 25, 190–196. doi:10.1007/s003480050223

Pankow, J.F., Asher, W.E., List, E.J., 1984. Carbon Dioxide Transfer at the Gas/Water Interface as a Function of System Turbulence, in: Gas Transfer at Water Surfaces. Springer Netherlands, Dordrecht, pp. 101–111. doi:10.1007/978-94-017-1660-4_10

Someya, S., Bando, S., Song, Y., Chen, B., Nishio, M., 2005. DeLIF measurement of pH distribution around dissolving CO2 droplet in high pressure vessel. Int. J. Heat Mass Transf. 48, 2508–2515. doi:10.1016/j.ijheatmasstransfer.2004.12.042

Stöhr, M., Schanze, J., Khalili, A., 2009. Visualization of gas–liquid mass transfer and wake structure of rising bubbles using pH-sensitive PLIF. Exp. Fluids 47, 135–143. doi:10.1007/s00348-009-0633-6

Tsuchiya, K., Ishida, T., Saito, T., & Kajishima, T. (2003). Dynamics of Interfacial Mass Transfer in a Gas-Dispersed System. The Canadian Journal of Chemical Engineering, 81(August), 647–654.

Valiorgue, P., Souzy, N., Hajem, M. El, Hadid, H. Ben, Simoëns, S., 2013. Concentration measurement in the wake of a free rising bubble using planar laser-induced fluorescence (PLIF) with a calibration taking into account fluorescence extinction variations. Exp. Fluids 54, 1501. doi:10.1007/s00348-013-1501-y

Kong, G., Buist, K. A., Peters, E. A. J. F., & Kuipers, J. A. M. (2018). Dual emission LIF technique for pH and concentration field measurement around a rising bubble. Experimental Thermal and Fluid Science, 93, 186–194. https://doi.org/10.1016/j.expthermflusci.2017.12.032

Paul, M., Strassl, F., Hoffmann, A., Hoffmann, M., Schlüter, M., & Herres-Pawlis, S. (2018). Reaction systems for bubbly flows. European Journal of Inorganic Chemistry. https://doi.org/10.1002/ejic.201800146

Copyright Statement